J Mater Sci (2011) 46:2041–2049
DOI 10.1007/s10853-010-5036-9

Growth of multi-walled carbon nanotubes by catalytic decomposition of acetylene on Ni-supported carbon fibers prepared by the heat-treatment of cellulose fibers

**Namjo Jeong · Seong Ok Han · Heeyeon Kim ·
Hong-su Kim · Yun-jong You**

Received: 9 August 2010 / Accepted: 26 October 2010 / Published online: 11 November 2010

Abstract Cellular-type carbon fibers, prepared by heat-treatment of cellulose fibers that ranged from 500 to 2300 °C, were used as catalytic support for the growth of carbon nano-filaments. A comparison of the Raman spectra of products prepared at different heat-treatment temperatures showed significant variation in the carbon structure of the surfaces of the as-prepared carbon fibers. TEM observation clearly revealed that the products heat-treated below 1000 °C had an amorphous phase, and at 1500 °C they were similar to glassy carbon—an example of non-graphitizing carbon. Surface graphitization of the carbon fibers derived by pre-treatment at 1500 °C was accomplished at above 2000 °C. Multi-walled carbon nanotubes (MWCNTs), approximately 15 nm and 8 μm in diameter and length, were synthesized on the surface of the prepared carbon fibers via a tip growth mechanism. TEM images and Raman spectra confirmed that the higher synthesis temperature could lead to the formation of MWCNTs with better crystalline carbon shells.

Introduction

The conversion of cellulose to carbonaceous materials starts at about 300 °C [1]. It is well known that cellulose cannot be directly transformed into crystalline graphite even at temperatures as high as 3000 °C, which results in the formation of amorphous carbon or glassy carbon [2–4]. Recently, many techniques have been developed for the use of cellulose in the formation of surface-graphitized materials [5–7] such as graphite fiber, which is a high-strength material that is indispensable in modern materials technologies [8]—this remains a matter of debate, however, because of the need for high operating temperatures and resultant imperfect graphitic structures. On the other hand, non-graphitizing materials obtained from cellulose have a very high surface area and a mesoporous surface morphology [9], which makes them available for various applications such as an absorbent for hazardous gases and/or a support of catalysts for reduction reactions or catalytic growth of carbon nano-filaments such as carbon nanotubes (CNTs) and carbon nanofibers (CNFs).

Recent studies have reported the use of carbon-based substrates for the growth of carbon nano-filaments. Zhu et al. demonstrated the synthesis of CNTs on a carbon fiber-supported iron (Fe) catalyst using methane gas [10]. Li et al. controlled the growth of CNTs on graphite foil by chemical vapor deposition [11]. Also, De Riccardis et al. synthesized CNTs on carbon fiber coated with nickel nanoparticles using an electro-deposition, and explained the anchorage effect of the CNTs [12]. However, most of the carbon substrates used in the existing literature has been artificial material.

Biomass has many merits such as low price, easy acquisition, and especially various kinds and shapes. Therefore, preparation of carbon materials from the

---

Electronic supplementary material The online version of this article (doi:10.1007/s10853-010-5036-9) contains supplementary material, which is available to authorized users.

N. Jeong (✉) · S. O. Han (✉) · H. Kim · H. Kim · Y. You
Reaction and Separation Materials Research Center, Korea Institute of Energy Research, 71-2, Jang-dong, Yuseong-gu, Daejeon 305-343, Korea
e-mail: njjeong@kier.re.kr

S. O. Han
e-mail: sohan@kier.re.kr

biomass is very economical and facile. Also variety of the biomass in shape leads to the formation of unique carbon materials such as carbon fibers consisting of many microtubules in this work, resulting in the extended applications such as catalytic converter or electrode materials. In the present study, we obtained carbon fibers from the heat-treatment of henequén fiber, which is a natural cellulose material. A controlled heat-treatment temperature that ranged from 500 to 2300 °C was the main factor in the variation of the surface morphologies of the prepared carbon fibers. Nickel nanoparticles of approximately 10 nm, catalytic seeds for the growth of carbon nano-filaments, were formed on the surface of the prepared carbon fibers using dip-coating and reduction processes. As-synthesized carbon nano-filaments were multi-walled carbon nanotubes (MWCNTs), 15 nm and 8 μm in diameter and length, although some CNFs were synthesized at lower temperatures. Synthesis temperature had an important influence on the crystallinity of the carbon nano-filaments.

Experiments

Materials and heat-treatment

Henequén fiber (Agave *fourcroydes*) ranging in lengths from 60 to 70 cm, supplied by DESFITYSA (Desfibradora Yucateca, S.A.) of Mérida Yucatán, México, was used as the starting material. The average density was about 1.45 g/cm^3. Before heat-treatment, the diameters of the cellulose fibers ranged from 100 to 200 μm. The fibers were washed with distilled water for 30 min at room temperature and then dried at 100 °C for 24 h. For pre-treatment, the prepared cellulose fibers were heated to the desired temperature, which was controlled at between 500 and 1500 °C, under a supply of only H_2 using a general electric furnace. The furnace was heated at a rate of 12.5 °C/min for 1 h, and then cooled to room temperature. For graphitization, the carbon fibers prepared at 1500 °C were again heat-treated at above 2200 and 2300 °C.

Growth of carbon nano-filaments

For the growth of carbon nano-filaments after the heat-treatment, carbon fibers prepared at 700, 900, 1500, and 2300 °C, respectively, were soaked in a nickel nitrate solution (0.01 wt% in deionized water) and held for 30 min in an ultrasonic bath. The Ni-supported carbon fibers were completely dried at 100 °C and put into a quartz boat. For pre-conditioning, the samples were installed into the furnace and was reduced at 500 or 700 °C for 2 h in hydrogen (H_2) 20 vol.% in Argon (Ar) and then cooled to room temperature. For CNT growth, the furnace temperature was again raised at a rate of 10 °C/min to a synthesis temperature in the range of 550–850 °C and kept at this temperature for 1 h. Ar of 1000 cc/min was used as the carrier gas.

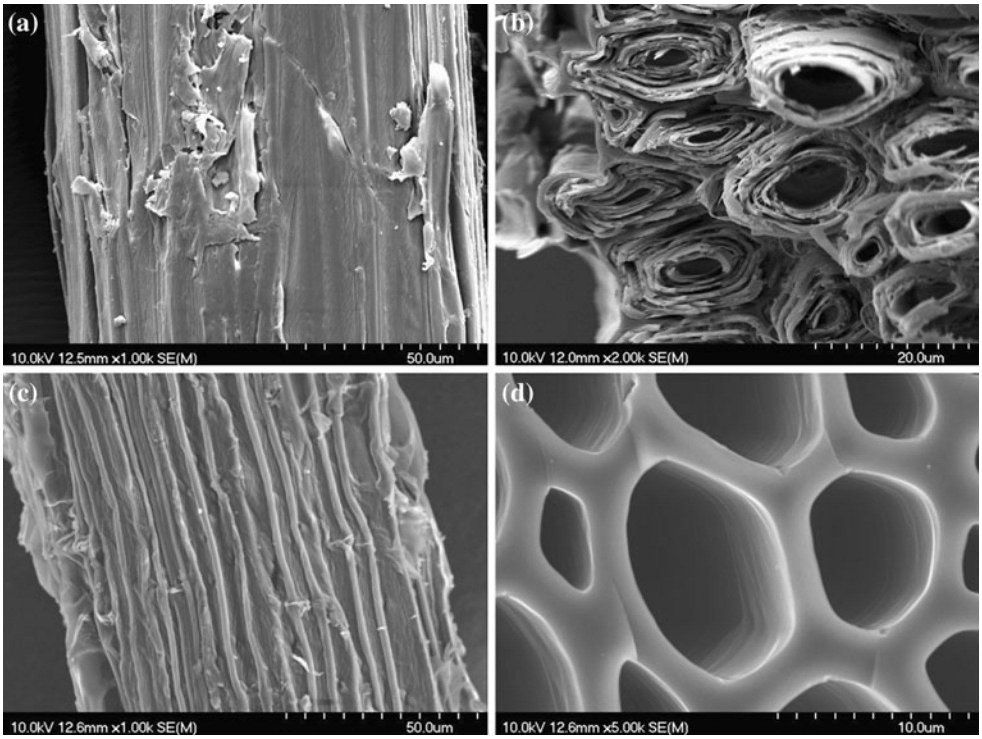

Fig. 1 Before (**a**, **b**) and after (**c**, **d**) heat-treatment of henequén fiber

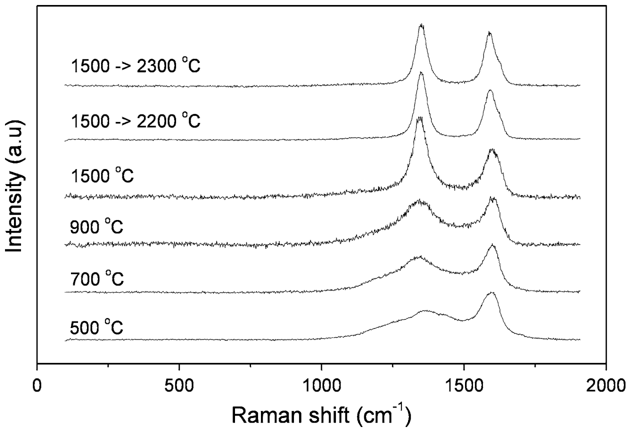

Fig. 2 Raman spectra of carbon fibers heat-treated for 1 h at 500, 700, 900, 1500, 2200, and 2300 °C. Note that heat-treatment at 2200 and 2300 °C was conducted using the carbon fibers pre-treated for 1 h at 1500 °C

Acetylene and H_2 of 20 and 10 cc/min, respectively, were additionally supplied into the furnace. Following the growth process, the furnace was cooled to room temperature in Ar.

Characterizations

Characterization of the obtained carbon fibers and MWCNTs was accomplished using field emission scanning electron microscopy (FE-SEM: HITACHI S-4700 operated at an accelerating voltage of 10 kV), high-resolution transmission electron microscopy (HRTEM: TEM-JEM 2000FXII operated at an accelerating voltage of 300 kV), Raman spectroscopy (LabRam HR with an Ar-ion laser 514 nm), TEM-energy dispersive X-ray spectroscopy (TEM-EDX: EDAX, Genesis), and N_2 adsorption measurement (Brunauer–Emmett–Teller (BET): ASAP 2010—Protech).

Results and discussion

Preparation of carbon fibers

Figure 1 shows the SEM images of henequén fiber before (a, b) and after (c, d) heat-treatment. Henequén

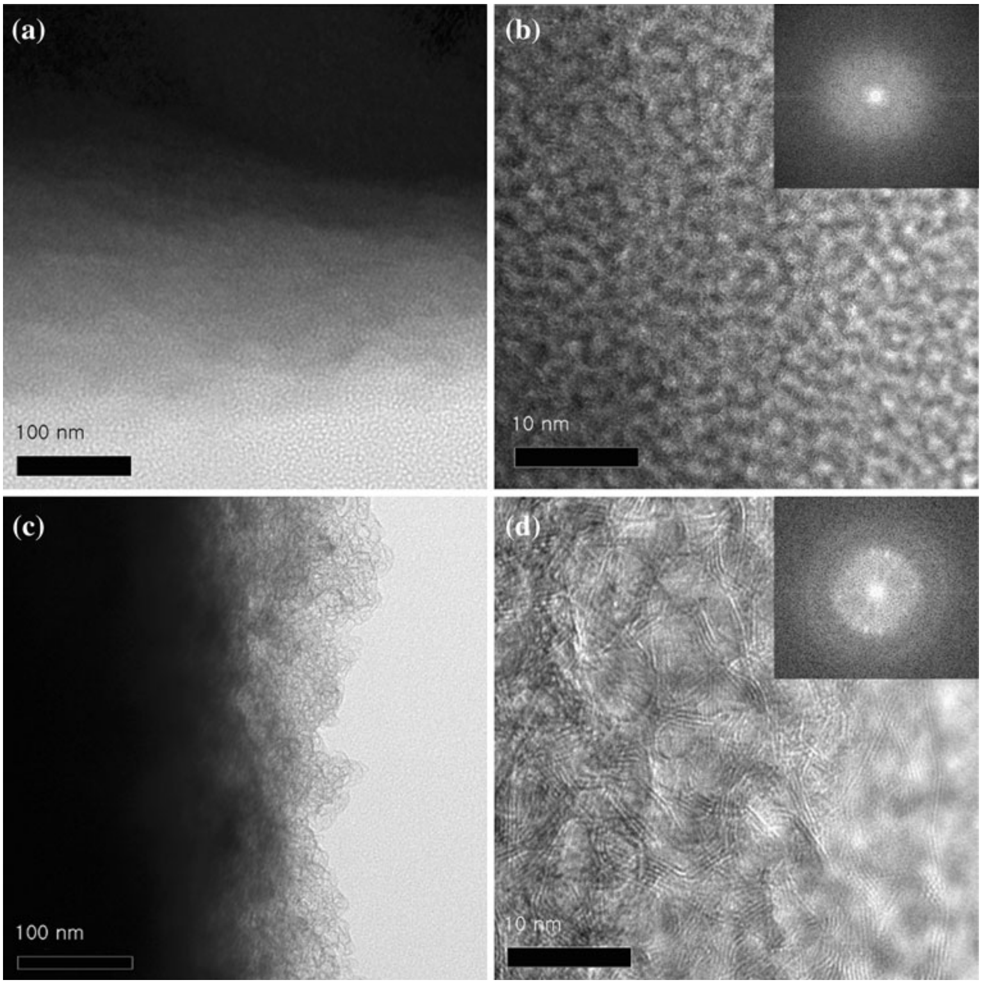

Fig. 3 TEM images of carbon fibers heat-treated for 1 h at 700 and 1500 °C. *Insets* of (**b**) and (**d**) show the SAED pattern of HRTEM images

fiber before heat-treatment had a smooth surface (a). Figure 1b shows many fabric layers on the cross section of the raw fiber. After heat-treatment, on the other hand, the fabric walls perfectly disappeared and a clean cellular structure appeared on the cross section of the obtained carbon fiber.

Figure 2 shows the Raman spectra of the carbon fibers prepared at temperatures of 500, 700, 900, 1500, 2200, and 2300 °C. Heat-treatments at 2200 and 2300 °C were conducted for 1 h with carbon fibers pre-treated at 1500 °C. Using given information on the average properties of a material, the Raman analysis is an effective method for characterizing carbon materials. In particular, the position and the intensity ratio of the G-line (assigned for the tangential stretching band of highly ordered graphite) and the D-line (demonstrating structural defects in the graphite crystals and the disorder-induced features) helps explain the atomic structure and size of carbonaceous materials [13]. Trends of the recorded spectra revealed that the sharpness of the D-line peaks detected at approximately 1350 cm^{-1} increased gradually as the heat-treatment temperature increased. The D-line peaks of the samples obtained below 900 °C, recorded at approximately 1590 cm^{-1}, appeared similar to those of a typical amorphous carbon [14]. On the other hand, the Raman spectrum of carbon fibers treated at 1500 °C revealed that the sharpness of the D-line peak was enhanced and the discrimination between G- and D-lines became clearer. This peak pattern has been observed from the surface of very disordered crystalline carbon [15] and also implies variation in the carbon structure of the surface of the heat-treated carbon fiber as heat-treatment temperature is increased. Heat-treatments conducted for 1 h at 2200 and 2300 °C after pre-treatment at 1500 °C showed the more obvious discrimination between G- and D-lines and a significant decrease in the intensity of the D-line peaks. This equates to an enhancement of the carbon crystallinity on the surface of the carbon fibers. These results could be explained by a change in the intensity ratio (I_D/I_G) related to amorphization and graphitization of the sample [16]. It is generally accepted that the I_D/I_G ratio can be determined by the ratio of peak heights or peak areas [17]. When variation of peak height or broadness is high, the ratio comparison with peak areas can be more useful for evaluating the effect of material ordering [18]. Herein, we utilized Lorentzian profiles as the simplest fits in order to compare the ratio of peak areas. The intensity ratios were 2.16, 1.21, and 1.13 for heat-treatment temperatures of 1500, 2200, and 2300 °C, respectively.

These variations shown in the Raman spectra were confirmed in the TEM images of as-prepared carbon fibers (Figs. 3, 4). As Fig. 3a and b shows the carbon fiber treated

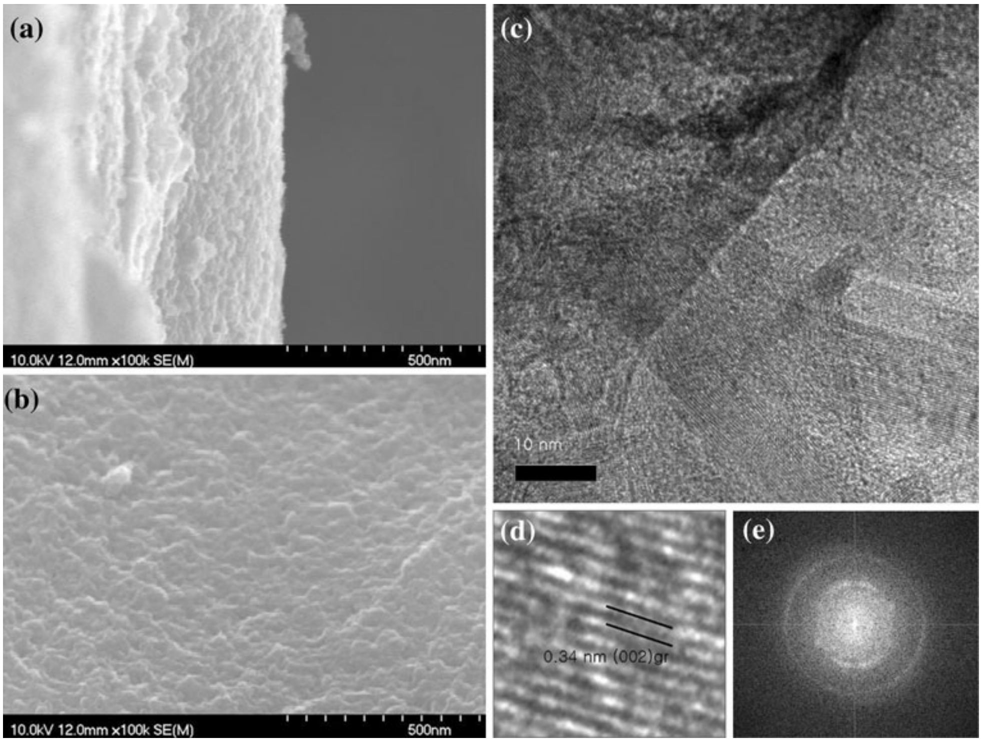

Fig. 4 SEM (**a**, **b**) and TEM (**c**) images of carbon fibers heat-treated for 1 h at 2200 °C after pre-treatment for 1 h at 1500 °C. **d** and **e** shows the HRTEM image and SAED pattern of (**c**), respectively. Note that lattice spacing of approximately 0.34 nm corresponding to the (0 0 2) lattice plane of bulk graphite was observed

at 700 °C was amorphous. This result is clearly verified by the selected area electron diffraction (SAED) pattern shown in Fig. 3b. When the henequén fiber was heat-treated at 1500 °C, however, a nanostructured carbon layer of approximately 100 nm was formed on the surface of the treated carbon fiber (Fig. 3c). The layer seemed to consist of pores bounded by curved or incompletely closed graphitic walls that consisted of two to four carbon layer planes approximately 4 nm in size (Fig. 3d). Obviously closed carbon nanostructures, such as hexagonal carbon nanoparticles or heptagonal carbon rings, could be partially found in this product (Fig. 3d and its inset). The surface structure of the carbon fiber treated at 1500 °C was similar to that of glassy carbon, which is an example of non-graphitizing carbon [19].

On the surface graphitization of henequén fiber-derived carbon, we tried to re-heat-treat the carbon fibers prepared at 1500 °C. The high-resolution SEM images of the surface of the 2200 °C-treated carbon fiber and the cross section perpendicular to the carbon fiber axis are shown in Fig. 4a and b. A typical granular texture [20, 21] was observed on the surface of the carbon fiber. The uneven surface seemed to consist of many protrusions ranging from 50 to 100 nm. Figure 4c shows the formed graphite layer skin. The HRTEM image (Fig. 4d) clearly reveals that the main lattice spacing was approximately 0.34 nm, as assigned to (0 0 2) the plane of the bulk graphitic carbon. The SAED pattern strongly supports these results (Fig. 4e). Therefore, it seems plausible to suggest that the surface of the carbon fibers re-treated at 2200 °C consisted of a thin graphite layer formed on the inside surface corresponding to a granule texture.

The BET surface area of the carbon fibers heat-treated at temperatures of 500, 700, 900, and 1500 °C was approximately 242, 321, 381, and 70 m^2/g, respectively. Evaluation of the formed pore sizes showed a range from 2 to 10 nm.

Growth of carbon nano-filaments

Figure 5 shows Ni nanoparticles formed on the surface of the carbon fibers treated at 900 °C. As-formed Ni nanoparticles, approximately 10 nm in average diameter (Fig. 5b), were well-dispersed on the surface of the carbon fibers. The HRTEM image and the SAED pattern (Fig. 5c, d) clearly identified the (1 1 1) plane assigned to a lattice

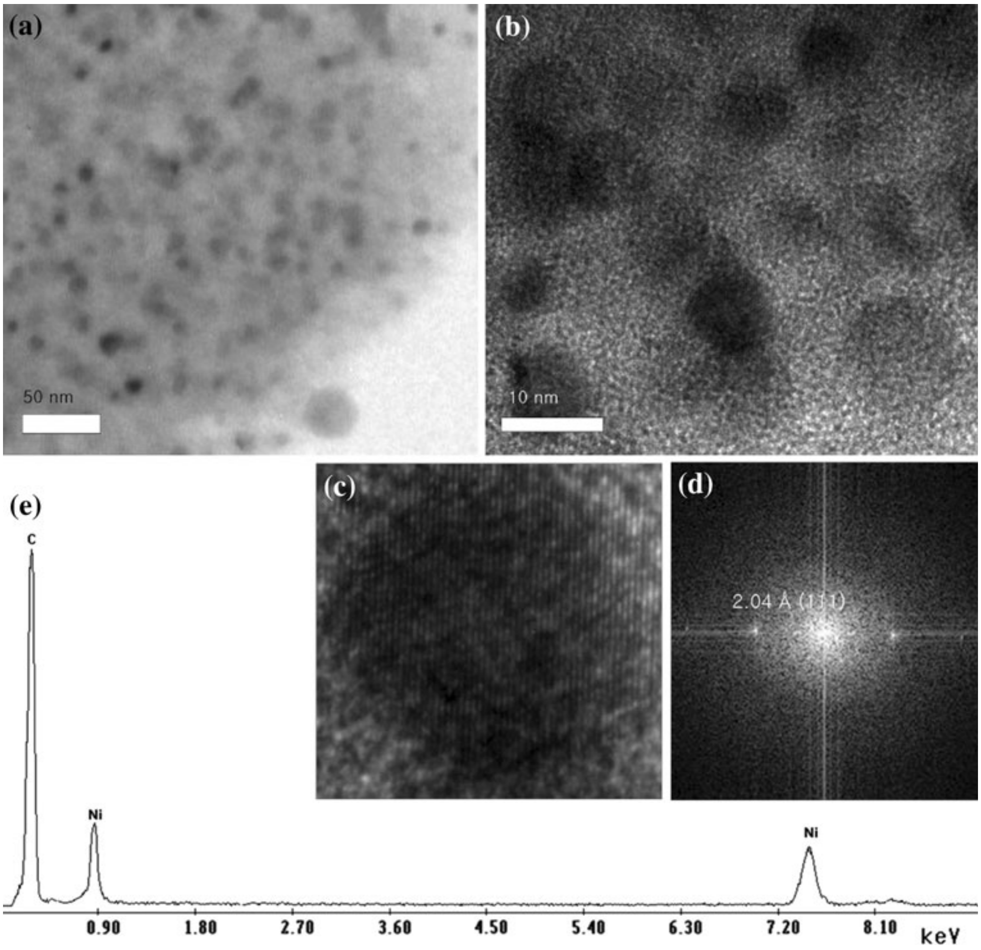

Fig. 5 TEM images (**a**, **b**) of Ni nanoparticles dispersed on the surface of the carbon fibers heat-treated at 900 °C. **c** and **d** shows the HRTEM image and the SAED pattern of a Ni nanoparticle selected in (**b**). **e** shows the EDX spectrum of Ni nanoparticles formed on the surface of the prepared carbon fibers

spacing of 0.204 nm. The EDX spectrum supported the formation of pure Ni nanoparticles on the surface of the prepared carbon fibers.

Figure 6a and b shows the SEM images of the surfaces of the carbon fiber after the growth of carbon nano-filaments at 700 °C. The used carbon fibers were prepared at

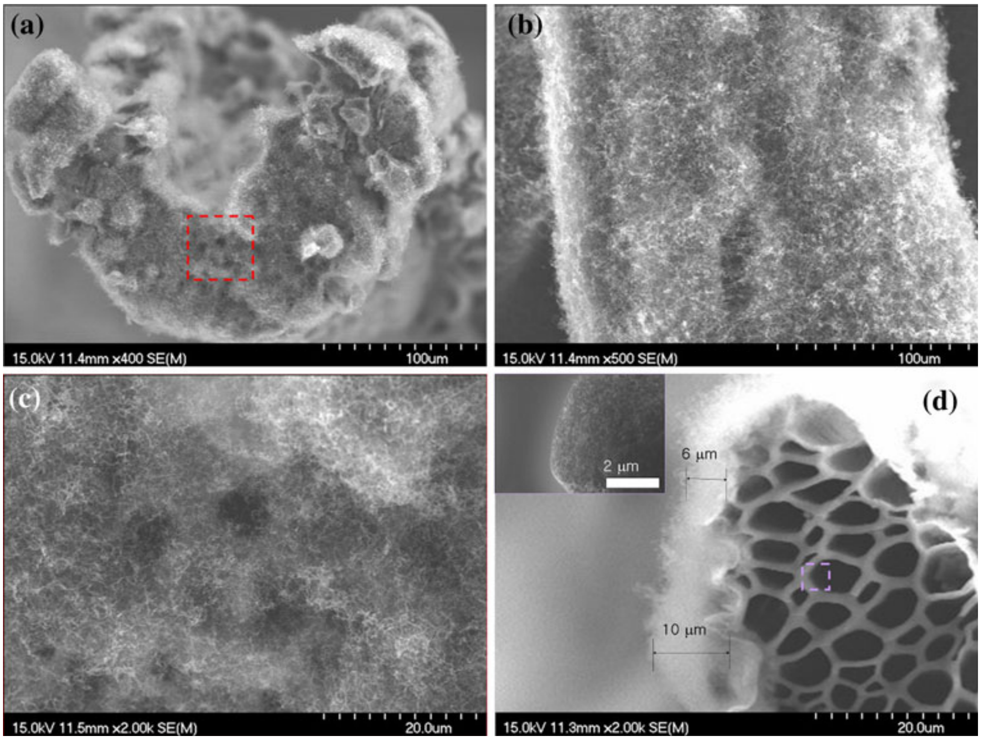

Fig. 6 SEM images of carbon nano-filaments grown on the surface of carbon fibers heat-treated at 900 °C. The carbon nano-filaments were synthesized for 1 h at 700 °C. *Inset* of (**d**) shows the carbon nano-filaments grown on the internal surface of the microtubules that formed on the cross section of the prepared carbon fibers

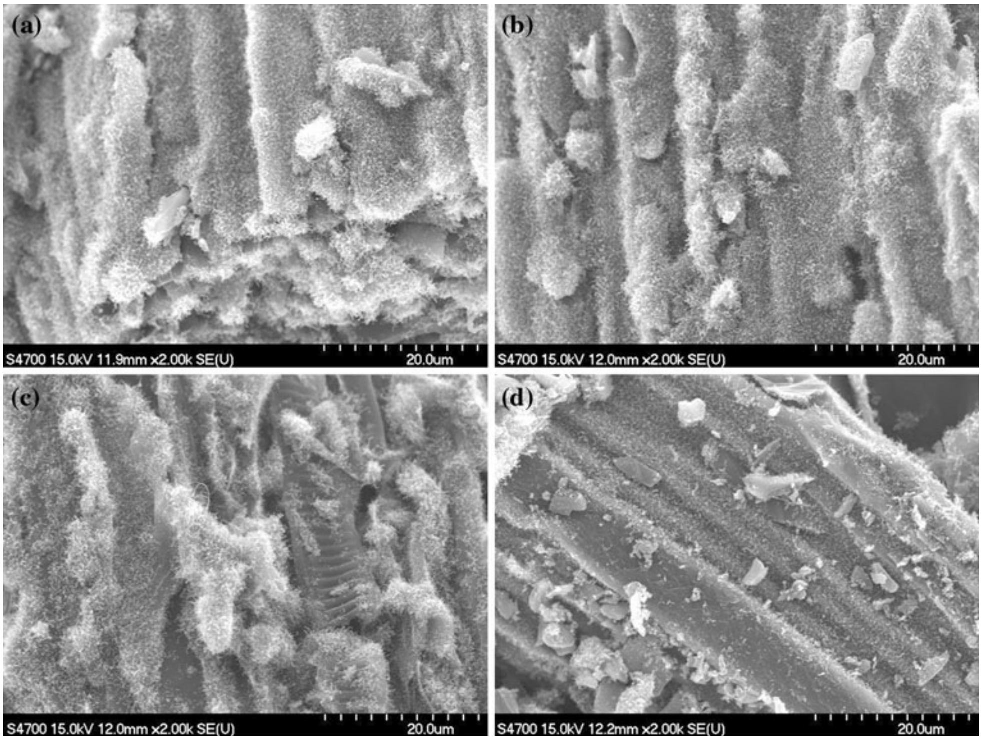

Fig. 7 SEM images of carbon nano-filaments grown on the surface of carbon fibers heat-treated at **a** 700, **b** 900, **c** 1500, and **d** 2300 °C, respectively. The growth of carbon nano-filaments was conducted for 30 min

900 °C. Figure 6c shows the high-resolution SEM image of the selected area proving that the surface of the carbon fiber was perfectly covered with as-synthesized carbon nano-filaments. The carbon nano-filaments appeared wavy and had regular diameters. The length of the carbon nano-filaments ranged from 6 to 10 μm (Fig. 6d). The inset of Fig. 6d shows that some carbon nano-filaments appeared on the internal surface of the microtubules formed on the cross section of the prepared carbon fibers. However, the growth yield of carbon nano-filaments was more significant on the external surface of the carbon fiber than on the inside of the microtubules.

Figure 7 shows the SEM images of carbon nano-filaments grown for 30 min on the carbon fibers heat-treated at 700, 900, 1500, and 2300 °C, respectively. The surface of carbon fibers treated at 700 and 900 °C was completely covered with carbon nano-filaments. However, growth yield of the carbon nano-filaments decreased as increase of

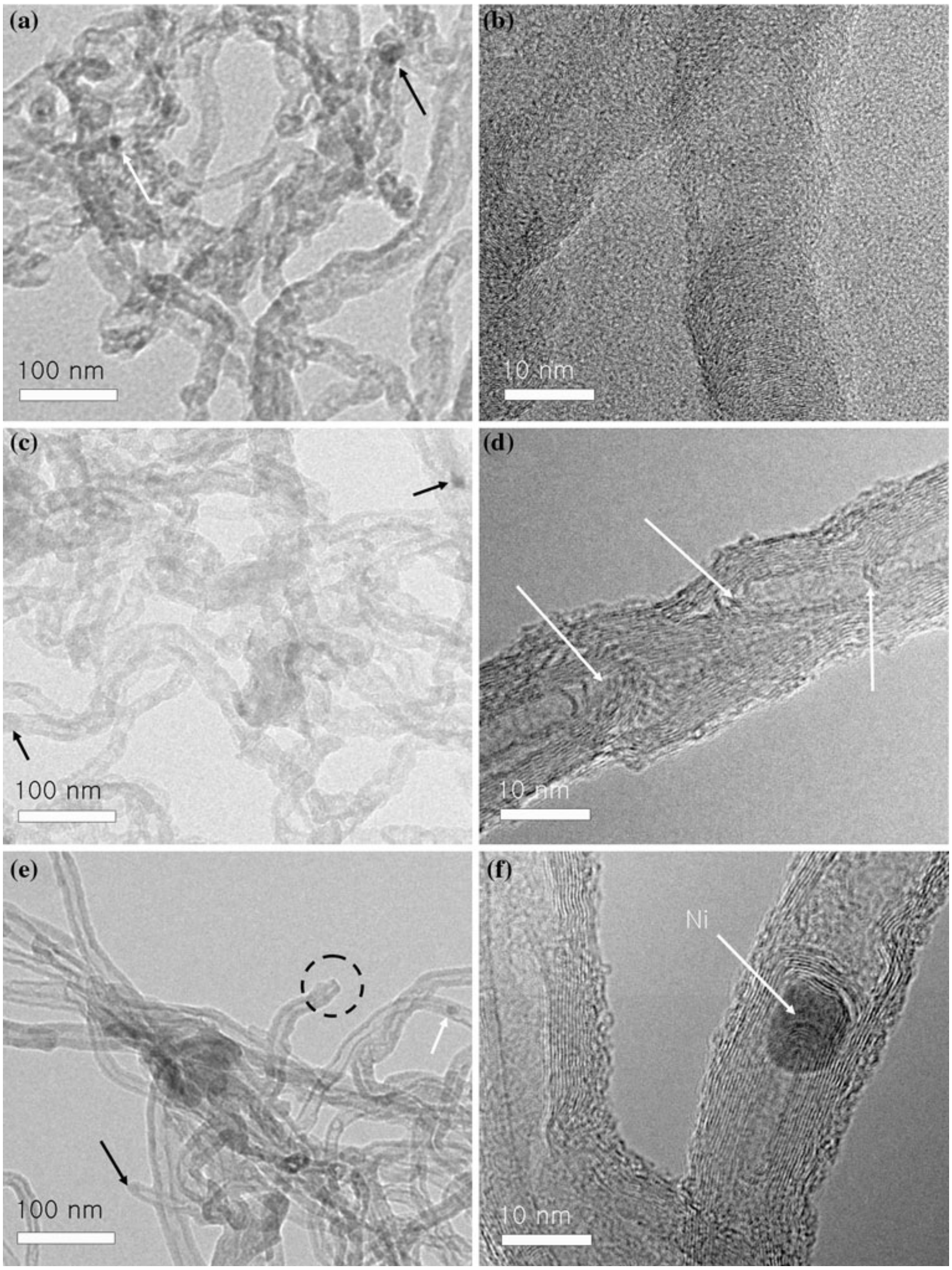

Fig. 8 TEM images of the carbon nano-filaments grown for 1 h at 550 (**a**, **b**), 700 (**c**, **d**), and 850 (**e**, **f**) °C. *Arrows* in (**a**, **c**, **e**, and **f**) indicate the Ni nanoparticles encapsulated in the carbon nano-filaments. *Arrows* in (**d**) indicate compartment layers formed in the inside cavity of the carbon nano-filaments. The *circle* in (*e*) shows the open-ended root of a CNT without a Ni nanoparticle

heat-treatment temperature. Decrease of coverage of carbon nano-filaments was remarkable on the surface of carbon fibers prepared at 2300 °C. This trend can be explained from the results shown in Figs. 3 and 4. Increase of heat-treatment temperature leads to the phase change of amorphous carbon surface into crystalline that results in the appearance of hydrophobic surface on carbon fibers. Wettability of nickel hydrate solution on the hydrophobic surface of the carbon fibers gets worse. This means that nickel nanoparticles, seeds of nanofilaments growth, can be sparsely formed on the surface. Therefore, it can be suggested that growth yield of carbon filaments on carbon fibers comparably depends on the correlation of the surface morphologies of the substrate and the used catalytic solution.

Figure 8a and b, TEM images of samples obtained at 550 °C, shows the wavy carbon nano-filaments. The cavities inside the nano-filaments were either very narrow or non-existent. The walls were not parallel to the growth direction of the carbon nano-filaments. The average outer diameter of the carbon nano-filaments was approximately 15 nm (Fig. 8b). The shape of these carbon nano-filaments was similar to a herringbone-type CNF [22]. In Fig. 8c and d, the arrows indicate Ni nanoparticles enclosed in the CNFs. At 700 °C, Ni nanoparticles were observed at the tip and stem of the carbon nano-filaments (arrows of Fig. 8c). Most carbon nano-filaments looked like CNTs, having compartment layers inside the cavity (Fig. 8c and arrows of Fig. 8d). A few CNTs were observed with a well-hollowed cavity. The CNTs were MWCNTs with outer diameters of approximately 15 nm. When synthesis temperature was increased to 850 °C (Fig. 8e, f), as-synthesized carbon nano-filaments were mostly well-crystallized with outer diameters of approximately 15 nm. Ni nanoparticles were found at both the tip (black arrow of Fig. 8e) and the stem (white arrows of Fig. 8e, f) of the CNTs. The circle in Fig. 8e shows the open-ended root of a CNT with no Ni nanoparticle. The positions of these Ni particles showed that the tip growth mechanism had the primary responsibility for the growth of carbon filaments.

The TEM results mentioned can be clearly demonstrated by Raman analysis (Fig. 9). In the first-order Raman spectrum for as-formed carbon nano-filaments, the prepared samples have main peaks at approximately 1352 (D-line) and 1585 cm^{-1} (D-line) [23]. The intensity ratios (I_D/I_G ratio) for peak areas were 2.08, 1.14, and 0.75 at synthesis temperatures of 550, 700, and 850 °C, respectively. At 550 °C, an inflection point was clearly detected at the tail of the G-line, approximately 1620 cm^{-1} (D′-line), suggesting there were defects in the carbon crystalline [24]. Strong features of the D′-line peak dwindled away with an increase in the synthesis temperature. The I_D/I_G ratio increased as the synthesis temperature decreased. This implies that the crystallinity of the carbon nano-filaments obtained at 850 °C was better than that at lower temperature. This result became clearer in the second-order Raman spectrum, where the peaks appeared mostly around 2460, 2705 (G′-line), 2947 (D + G-line), and 3251 cm^{-1} (2D′-line). A higher synthesis temperature, at the 2705 cm^{-1} (G′-line) peak, meant better crystallinity of CNTs as it became stronger. The $I_{D+G}/I_{G'}$ ratios for peak areas were 0.84, 0.35, and 0.1 at synthesis temperatures of 550, 700, and 850 °C, respectively. These evaluations were consistent with those of the I_D/I_G ratio. Consequently, it was suggested that a high synthesis temperature could lead to the growth of well-graphitized carbon nano-filaments [25].

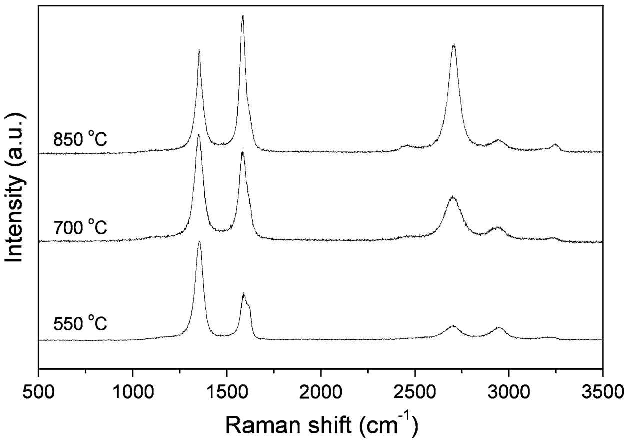

Fig. 9 Raman spectra of carbon nano-filaments grown for 1 h at 550, 700, and 850 °C. The recorded spectra ranged from 100 to 4000 cm^{-1}

Conclusion

Carbonization and surface graphitization of henequén fiber were successfully conducted in heat-treatment that ranged from 500 to 2300 °C. Heat-treatment between 500 and 900 °C showed that as-produced carbon fibers had an amorphous phase. With heat-treatment of 1500 °C, a glassy carbon layer of approximately 100 nm was found on the surface of the treated carbon fibers. The layer seemed to consist of incomplete nanostructures with pores approximately 4 nm in size. Surface graphitization of the carbon fibers was derived from henequén fiber at 1500 °C, and could be accomplished at above 2000 °C.

In addition, we tried to grow carbon nano-filaments on the surface of the heat-treated carbon fibers. As-synthesized carbon nano-filaments had a diameter and length of approximately 15 nm and 8 μm. Most carbon nano-filaments were MWCNTs grown via a tip growth mechanism, although formation of CNFs was observed at a lower temperature. TEM images and Raman spectra showed that the crystallinity of as-synthesized carbon nano-filaments enhanced as increase of the synthesis temperature.

Acknowledgements The authors thank Kwang-sik Myung (the Korea Institute of Energy Research: KIER) for the SEM analysis, and also Yun-chang Park (the National Nano Fab Center: NNFC) for the TEM analysis. This work was supported by the KIER (A9-2423).

References

1. Bacon R, Tang MM (1964) Carbon 2:221
2. Jenkins GM, Kawamura K (1971) Nature 231:175
3. Tang MM, Bacon R (1964) Carbon 2:211
4. Hishiyama Y, Yoshida A, Kaburagi Y (1993) Carbon 31:1265
5. Mitchell SJ, Thomas CR (1971) Carbon 9:253
6. Mathieu LM (1984) Carbon 22:521
7. Tanabe Y, Yamanaka J, Hoshi K, Migita H, Yasuda E (2001) Carbon 39:2347
8. Kim DY, Nishiyama Y, Wada M, Kuga S (2001) Carbon 39:1051
9. Titirici MM, Thomas A, Yu SH, Müller JO, Antonietti M (2007) Chem Mater 19:4205
10. Zhu S, Su C, Lehoczky SL, Muntele I, Ila D (2003) Diamond Relat Mater 12:1825
11. Li WZ, Wang DZ, Yang SX, Wen JG, Ren ZF (2001) Chem Phys Lett 335:141
12. Riccardis MF, Carbone D, Makris TD, Giorgi R, Lisi N, Salernitano E (2006) Carbon 44:671
13. Zhang Z, Dewan C, Kothari S, Mitra S, Teeters D (2005) Mater Sci Eng B 116:363
14. Casiraghi C, Ferrai AC, Robertson J (2005) Phys Rev B 72:85401-1
15. Gohier A, Minea TM, Point S, Mevellec JY, Jimenez J, Djouadi MA, Granier A (2009) Diamond Relat Mater 18:61
16. Urbonaite S, Hälldahl L, Svensson G (2008) Carbon 46:1942
17. Ferrai AC, Robertson J (2000) Phys Rev B 61:14095
18. Jeong N, Lee J (2008) J Catal 260:217
19. Harris PJF (2004) Philos Mag 84:3159
20. Yoshida A, Kaburagi Y, Hishiyama Y (1991) Carbon 29:1107
21. Kaburagi Y, Hosoya K, Yoshida A, Hishiyama Y (2005) Carbon 43:2817
22. Ren WC, Cheng HM (2002) Carbon 41:1657
23. Wang Z, Huang X, Xue R, Chen L (1998) J Appl Phys 84:227
24. Ni ZH, Fan HM, Fan XF, Wang HM, Zheng Z, Feng YP, Wu YH, Shen ZX (2007) J Raman Spectrosc 38:1449
25. Lee Y, Kim N, Park J, Han J, Choi Y, Ryu H, Lee H (2003) Chem Phys Lett 372:853